THE SOFTENING IN PLASTIC DEFORMATION OF METAL

Truong Tich Thien
University of Technology, VNU-HCM

1. INTRODUCTION

The nucleation, growth and coalescence of small internal voids or cavities are the microscopic mechanism of ductile fracture in cold forming processes of metal. The microvoids are nucleated under the tensile loading state at the impurities and hard particles in the ductile metal. After nucleated microvoids, they will be grown due to plastic deformation and coalesced together in order to create the microscopic ductile fracture when the critical state is reached. The nucleation and growth of small internal voids or cavities are interpreted as the reason of the strain softening of material. So, the strain hardening and the strain softening of material are two phenomena occurring simultaneously during the plastic deformation of materials. At first the strength of material increases since the strain hardening, but the material will be degraded due to the growth of microvoids. This induces the strength degradation and the stress−strain relationship will be shown by the curve with the negative slope.

The initial shapes of micro-voids are multiform and complex. On the other hand, their distribution is random and difficult to determine. For the feasibility of analysis model, two initial assumptions were proposed. Firstly, the initial shapes of micro-voids are supposed the cylinder with circular cross section in two-dimensional problems and the sphere in three-dimensional problems (fig. 3). Finally, these voids are uniformly arrayed in material.

The chief goal of this paper is to examine the growth of voids and the strain softening of structure inside the ductile metal with the initial spherical voids and uniform distribution in cold forming processes of metal. The numerical results are obtained by two models: the analytical model and the finite element model. There is a good agreement between the results of proposed model and experiments.

2. COMPUTING MODELS

2.1. The analytical model

2.1.1. Nucleation of voids

The impurities and hard particles always exist in technical ductile metals (fig.1) and the concentrated stress at these loci will be the reason to form micro-voids (fig.2). These voids are nucleated at the particle-matrix interface due to the agglutinate loss or the particle crack.

Enlarge 415 Enlarge 2000

Figure 1. Types of manganese sulphide particles in steel.

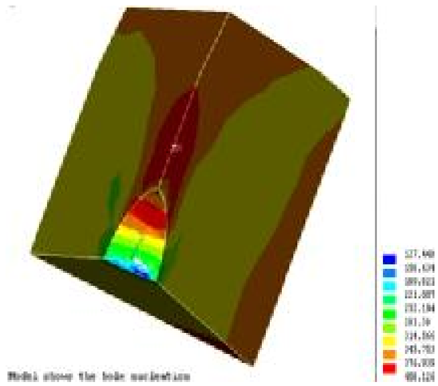

Figure 2.The concentrated stress at two poles of hard particle

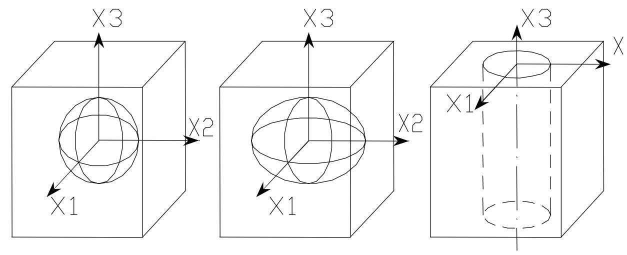

Figure 3. Types of voids in model.

2.1.2. Analytical model for growth of voids

Mc.Clintock (1968) developed firstly a model for growth of cylindrical void in strain hardening materials. An isolated cylindrical void (with longitudinal axis c, semi-axes a and b) will be changed according to

$$\ln\left(\frac{R}{R_0}\right)=\frac{\sqrt{3}\varepsilon_e}{2(1-n)}\sinh\left[\frac{\sqrt{3}(1-n)}{2}\frac{(\sigma_a+\sigma_b)}{\sigma_{eM}}\right]+\frac{\varepsilon_a+\varepsilon_b}{2} \quad (1)$$

For a material cell with several series of cylindrical voids (fig.4), interaction of neighbouring void must be introduced in the model of void growth. At a uniform void distribution (initial void distances), the growth parameters in radial direction a and b are defined according to

$$\mathbf{l}_a^0,\ \mathbf{l}_b^0,\ \mathbf{l}_c^0$$

$$F_{ca}=\frac{a}{a_0}\frac{\mathbf{l}_a^0}{\mathbf{l}_a} \quad \text{and} \quad F_{cb}=\frac{b}{b_0}\frac{\mathbf{l}_b^0}{\mathbf{l}_b} \quad (2)$$

Under all-round tension, voids are grown increasingly faster than the forced strain, according to the equations obtained from Levy-von Mises

$$d(\ln F_{ca})=\left\{\frac{\sqrt{3}}{2(1-n)}\sinh\left[\frac{\sqrt{3}(1-n)}{2}\frac{(\sigma_a+\sigma_b)}{\sigma_{eM}}\right]+\frac{3}{4}\frac{\sigma_b-\sigma_a}{\sigma_{eM}}\right\}d\varepsilon_e \quad (3a)$$

$$d(\ln F_{cb})=\left\{\frac{\sqrt{3}}{2(1-n)}\sinh\left[\frac{\sqrt{3}(1-n)}{2}\frac{(\sigma_a+\sigma_b)}{\sigma_{eM}}\right]+\frac{3}{4}\frac{\sigma_a-\sigma_b}{\sigma_{eM}}\right\}d\varepsilon_e \quad (3b)$$

where σ_{eM} means the equivalent stress of material matrix.

The void initiation and effects of necking are not involved in the fracture criterion of Mc.Clintock. For this reason, the predicted fracture strain of a material is normally larger than the experimental value.

Thus, an improvement of Mc.Clintock is necessary. Nguyen Luong Dung modified the original Mc.Clintock model by adding a second model, fig.4c, to the original model, fig.4b, with

$$\sigma_a^*=-\left(\frac{\sigma_a+\sigma_b}{2}-\sigma_a\right) \quad \text{and} \quad \sigma_b^*=-\left(\frac{\sigma_a+\sigma_b}{2}-\sigma_b\right) \quad (4)$$

The growth parameters in radial direction a and b of modified model are now defined according to

$$F_{ca} = \frac{R_a}{R_0}\exp\left(2\varepsilon_a^* - \varepsilon_a\right) \tag{5a}$$

$$F_{cb} = \frac{R_b}{R_0}\exp\left(2\varepsilon_b^* - \varepsilon_b\right) \tag{5b}$$

The accumulated damage rates of modified model in radial direction a and b are approximately given as

$$d\left(\ln F_{ca}\right) = \left\{\frac{\sqrt{3}}{2(1-n)}\sinh\left[\frac{\sqrt{3}(1-n)}{2}\frac{\left(\sigma_a+\sigma_b\right)}{\sigma_{eM}}\right] + \frac{3}{4}\frac{\sigma_a-\sigma_b}{\sigma_{eM}}\right\}d\varepsilon_e = f_{ca}d\varepsilon_e \tag{6a}$$

$$d\left(\ln F_{cb}\right) = \left\{\frac{\sqrt{3}}{2(1-n)}\sinh\left[\frac{\sqrt{3}(1-n)}{2}\frac{\left(\sigma_a+\sigma_b\right)}{\sigma_{eM}}\right] + \frac{3}{4}\frac{\sigma_b-\sigma_a}{\sigma_{eM}}\right\}d\varepsilon_e = f_{cb}d\varepsilon_e \tag{6b}$$

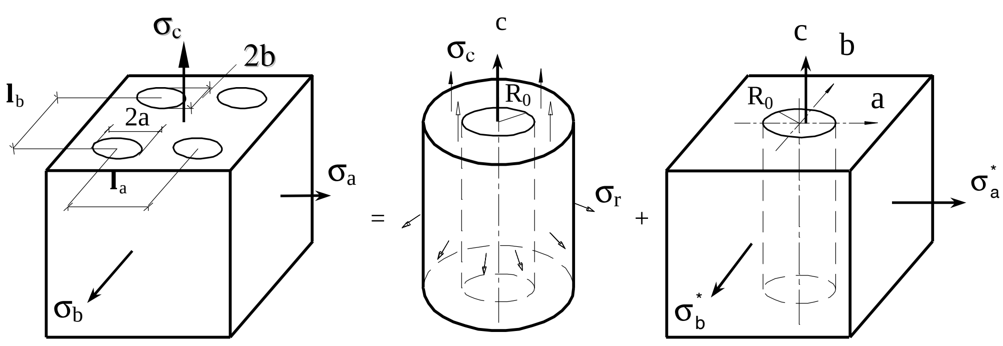

Figure 4. Modified model.

The other expressions for $d(\ln F_{ab})$ and $d(\ln F_{ac})$ or $d(\ln F_{ba})$ and $d(\ln F_{bc})$ will be obtained in the same way as equality (6).

In case of a material cell containing spherical voids as fig.3, the growth of a single spherical void, fig.5, is taken into account in order to analyze the fracture initiation. The rate of change of shape may be obtained if the spherical surfaces concentric with the void assume to become ellipsoids.

The accumulated damage rate of the momentary semi-axis a is extrapolated from (6a) and (6b) for a cylindrical void by means of a superposition method, fig.6, and is given as (7a). Generally, the accumulated damage rate of the momentary semi-axis i is given as (7b).

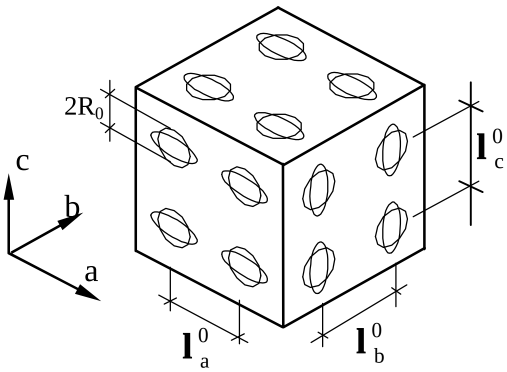

Figure 5. A cell of material.

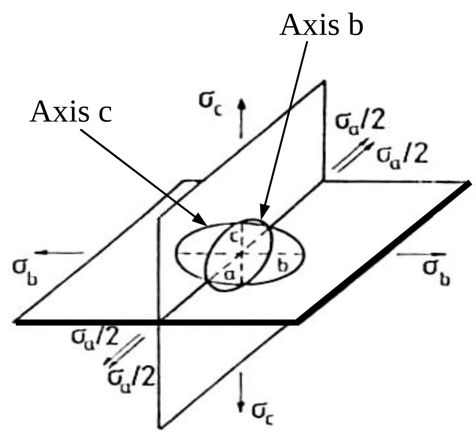

Figure 6. Growth of ellipsoid void.

$$
\begin{aligned}
d(\ln F_a) &= \left[\left\{\frac{\sqrt{3}}{2(1-n)}\sinh\left[\frac{\sqrt{3}(1-n)}{2}\frac{(\sigma_a/2+\sigma_b)}{\sigma_{eM}}\right]+\frac{3}{4}\frac{\sigma_a/2-\sigma_b}{\sigma_{eM}}\right\}+\right.\\
&\quad \left.+\left\{\frac{\sqrt{3}}{2(1-n)}\sinh\left[\frac{\sqrt{3}(1-n)}{2}\frac{(\sigma_a/2+\sigma_c)}{\sigma_{eM}}\right]+\frac{3}{4}\frac{\sigma_a/2-\sigma_c}{\sigma_{eM}}\right\}\right]d\varepsilon_e = \\
&= \left[\left\{\frac{\sqrt{3}}{(1-n)}\sinh\left[\frac{\sqrt{3}(1-n)}{4}\frac{\sigma_a+\sigma_b+\sigma_c}{\sigma_{eM}}\right]\cosh\left[\frac{\sqrt{3}(1-n)}{4}\frac{\sigma_b-\sigma_c}{\sigma_{eM}}\right]\right\}+\right.\\
&\quad \left.+\frac{3}{4}\frac{\sigma_a-\sigma_b-\sigma_c}{\sigma_{eM}}\right]d\varepsilon_e = f_a d\varepsilon_e
\end{aligned}
\tag{7a}
$$

$$
\begin{aligned}
d(\ln F_i) &= \left[\left\{\frac{\sqrt{3}}{(1-n)}\sinh\left[\frac{\sqrt{3}(1-n)}{4}\frac{\sigma_i+\sigma_j+\sigma_k}{\sigma_{eM}}\right]\cosh\left[\frac{\sqrt{3}(1-n)}{4}\frac{\sigma_j-\sigma_k}{\sigma_{eM}}\right]\right\}+\right.\\
&\quad \left.+\eta\frac{\sigma_i-\sigma_j-\sigma_k}{\sigma_{eM}}\right]d\varepsilon_e = f_i d\varepsilon_e
\end{aligned}
\tag{7b}
$$

where $\ln F_i = \ln\left(\frac{R_i}{R_i^0}\right)$ and $\eta = \frac{3}{2}$ for the isolated void, $\ln F_i = \ln\left(\frac{R_i}{R_i^0}\frac{\mathbf{l}_i^0}{\mathbf{l}_i}\right)$ and $\eta = \frac{3}{4}$ for void in porous media.

The accumulated damage of the momentary semi-axis i due to void growth is given as

$$
\begin{aligned}
A_i = \ln F_i &= \int_{\varepsilon_e^N}^{\varepsilon_e}\left[\left(\frac{\sqrt{3}}{(1-n)}\sinh\left\{\frac{\sqrt{3}(1-n)}{4}\frac{(\sigma_i+\sigma_j+\sigma_k)}{\sigma_{eM}}\right\}\right.\right.\\
&\quad \left.\left.\cdot\cosh\left\{\frac{\sqrt{3}(1-n)}{4}\frac{(\sigma_j-\sigma_k)}{\sigma_{eM}}\right\}\right)+\eta\frac{\sigma_i-\sigma_j-\sigma_k}{\sigma_{eM}}\right]d\varepsilon_e = \int_{\varepsilon_e^N}^{\varepsilon_e} f_i d\varepsilon_e
\end{aligned}
\tag{8}
$$

The influence of void growth on material forming behaviour was considered by softening parameter of porous material σ_e/σ_{eM}. The general form of yield function for porous material is given by TRUONG Tich Thien

$$\phi\left(\sigma_{ij}, \sigma_{eM}, f\right) = \left(\frac{\sigma_e}{\sigma_{eM}}\right)^2 + B\cosh\left(A\frac{\sigma_e}{\sigma_{eM}}\right) - C = 0 \quad (9)$$

where σ_{eM} is the equivalent stress of matrix material (no voids), the factors A, B, C depend on the porosity f, state of applied stress and material property, according to the formulas

$$A = \left(1.616 - 0.866n\right)S_m;\ B = 2.5f;\ C = 1 + 1.625f^2 \quad (10)$$

with $S_m = \sigma_m/\sigma_e$.

The concentrated plastic deformation appears at critical state before neighbouring voids touch together. So, the coalescence of neighbouring voids or ductile fracture will be occurred in a plane perpendicular to the maximum growth direction i of void if the accumulated damage of the momentary semi-axis i satisfies the following condition

$$A_i = A_{if}^* = \beta \ln\left(\frac{1}{2}\sqrt[3]{\frac{4\pi}{3f_0}}\right), \quad \beta \le 1 \quad (11)$$

The process of micro ductile fracture prediction is shown in the flowchart of figure 7.

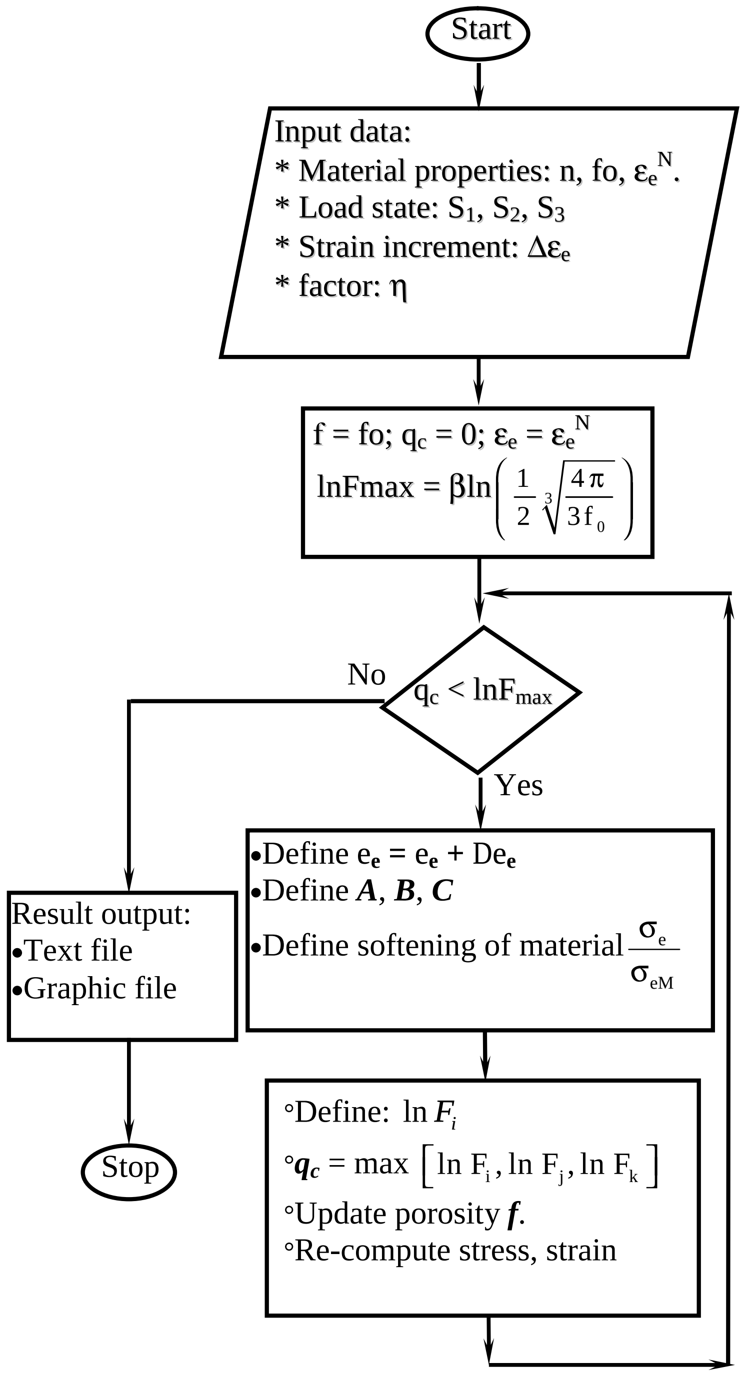

Figure 7. Flowchart of fracture prediction at a position.

2.2. The finite element model

For the symmetry, the FEM analysis model only includes one-sixteenth of material cell (fig.8).

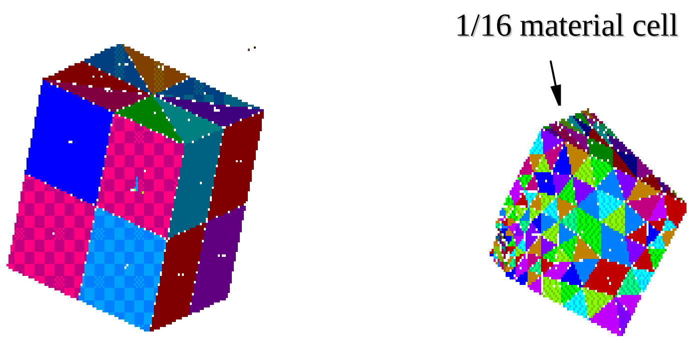

a) Material cell

b) FEM mesh

Figure 8. FEM Model

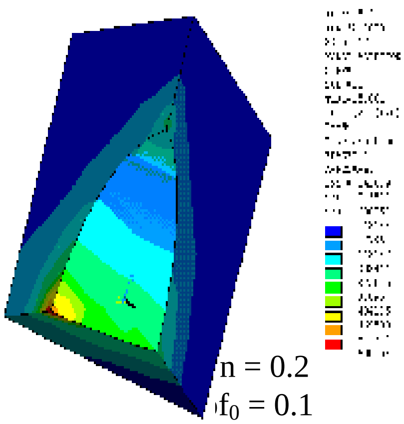

Figure 9a. Equivalent strain distribution of model.

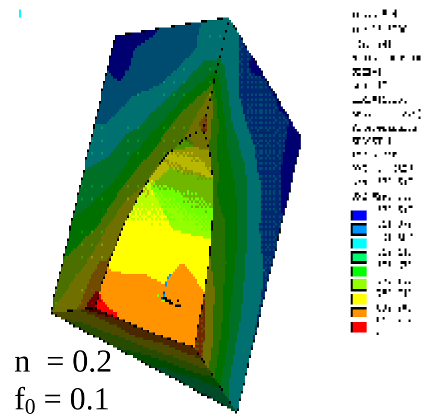

Figure 9b. Equivalent stress distribution of model.

Table 1. Load cases applied on cell

Load case	$\sigma_m/\sigma_e = S_m$	$\sigma_3/\sigma_e = S_3$	$\sigma_2/\sigma_e = S_2$	$\sigma_1/\sigma_e = S_1$
Axial load	1/3	1.0	0.0	0.0
Triaxial Load	1.25	1.9166	0.9166	0.9166
High triaxial Load	3.0	3.666	2.666	2.666

Two initial porous cases f_0 = 1% and f_0 = 10%, two types of material n = 0.1 and n = 0.2 and three load cases were computed (table 1).

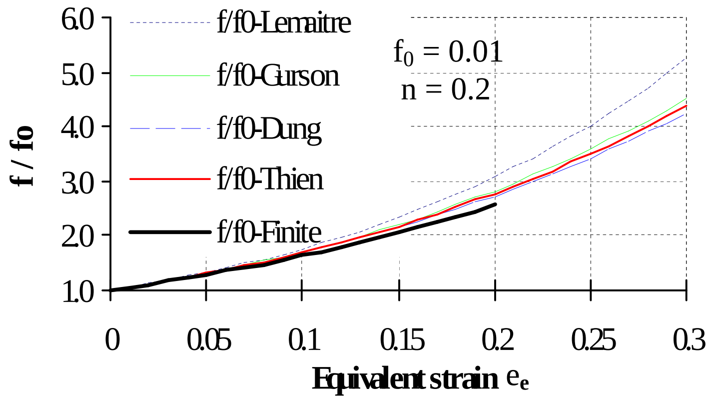

Figure 10. Porous variation according to different yield functions in triaxial load.

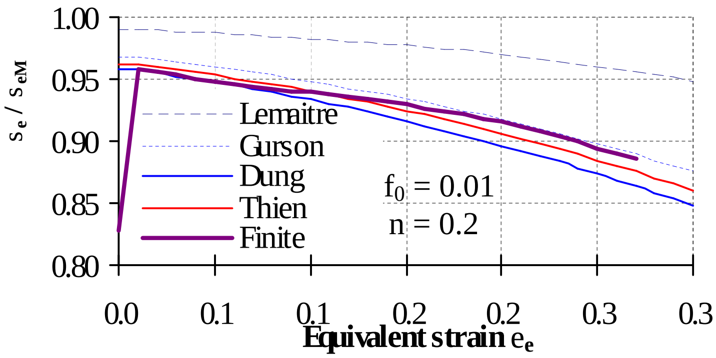

Figure 11a. Material softening according to different yield functions in triaxial load.

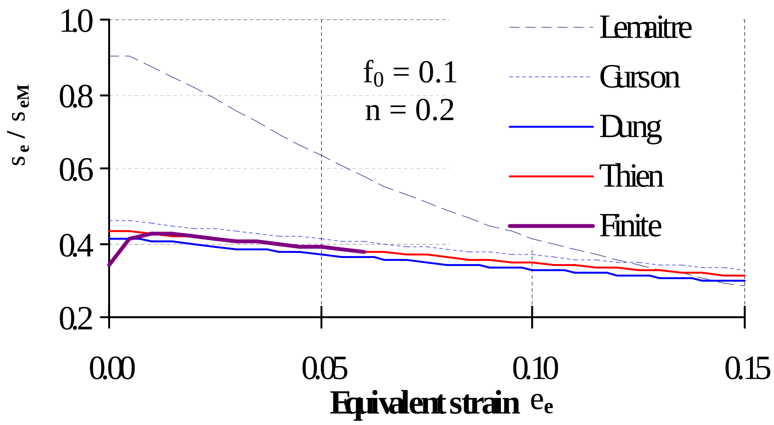

Figure 11b. Material softening according to different yield functions in high triaxial load.

Table 2. The fracture strain ε_{ef}

Steel	1015	1045	1090

Load / Yield function	Uni-Axia-lity	Tri-Axia-lity	High Tri-Axia-lity	Uni-Axia-lity	Tri-Axia-lity	High Tri-Axia-lity	Uni-Axia-lity	Tri-Axia-lity	High Tri-Axia-lity
Lemaitre	1.38	0.615	0.155	0.89	0.395	0.095	0.73	0.325	0.08
Gurson	1.39	0.65	0.405	0.89	0.46	0.35	0.73	0.4	0.33
Dung	1.39	0.66	0.42	0.91	0.49	0.425	0.75	0.45	0.425
Thien	1.39	0.655	0.415	0.9	0.475	0.39	0.74	0.425	0.375
Experiment	1.4			0.91			0.63		
Factor β	1			1			0.85		

The strain and stress results from FEM for a material sustained high triaxial load was shown on fig. 9a and fig. 9b.

The porous growth and material softening results from FEM were shown and compared with ones from analysis on fig.10, fig. 11. For every steel, the computational program exported the accumulated damage (fig.12) and fracture strains (table 2).

3. CONCLUSION

The developed model of the void growth takes into account both macro- and microscopic factors. This model is appropriate for the variation of the shape of ellipsoidal voids in a plastically deformed medium in cold forming processes of metal ($T < 0.4T_c$).

The growth and coalescence of voids depend on temperature of material, hydrostatic stress of load, … Under superposition of hydrostatic stress (negative stress), the growth of voids will be obstructed or delayed and the coalescence of void will not occur. This is an important method in order to avoid micro fracture in metal forming.

The void growth due to plastic deformation causes the softening and increases the accumulated damage of material. There is a good agreement between the results of proposed model and experiments. Thus, this predictive process gets promising future in metal forming.

REFERENCES

[1]. W. F. Chen, D. J. Han, *Plasticity for Structure Engineers*, Springer-Verlag- New York - Berlin - Heidelberg - London - Paris – Tokyo, (1988).

[2]. B. Dodd and Y. Bai, *Ductile Fracture and Ductility*, Academic Press, London (1987).

[3]. E. Doege, H. M. Nolkemper and I. Saeed, *Fliesskurvenatlas metallischer Werkstoffe*, Hanser Verlag, Muenchen (1986).

[4]. N. L. Dung, *Fortschr.- Ber. VDI Reihe 2 Nr. 175*, VDI-Verlag, Dusseldorf (1989).

[5]. T. T. Thien, *The Model for Ductile Fracture Prediction in Metal Forming*, Doctor Thesis, Ho Chi Minh City University of Technology, (07/2001).

[6]. Truong Tich Thien, Vu Cong Hoa, *A Process of Micro Ductile Fracture Prediction for Metal*, Proceedings of International Conference for Mechanical and Automotive Technologies (ICMAT) 2005, Chonbuk National University, Korea, June 1 ~ 3, (2005).

[7]. M. J. Worswick and R. J. Pick, *J. Mech. Phys. Solid 38*, 601 (1990).